Optical spectrum of a solid-state diode-pumped Fabry-Perot laser

P. A. Khandokhin, E. A. Ovchinnikov, and E. Yu. Shirokov
Institute of Applied Physics, Russian Academy of Science, 46 Ulyanov Street, 603600 Nizhny Novgorod, Russia
(Received 26 May 1999; published 12 April 2000)

In this paper we report an experimental and theoretical study of the joint effect of two types of longitudinal gain nonuniformity (partial cavity filling by an active medium and the exponential absorption of pump intensity along the active element) on competitive interaction of longitudinal modes. A justification of the approach to the description of solid-state laser dynamics with gain nonuniformity, where the dimension of the model is the same as in a simple case of uniform longitudinal gain distribution, is presented. A detailed comparison of different approaches to the problem of describing the longitudinal gain nonuniformity is made.

PACS number(s): 42.55 Ah, 42.55 Xi, 42.65 Sf

I. INTRODUCTION

The problem of the influence of spatially nonuniform gain profile on dynamical characteristics of solid-state lasers (optical spectrum, polarization, etc.) has a long history, especially as regards the relation between the longitudinal nonuniformity of gain and the lasing optical spectrum [1,2]. It was found that when an active medium is situated close to a cavity mirror, the competition of longitudinal modes is maximal and, as a result, an optical spectrum becomes rare: the gap between the lasing modes is more than one intermode frequency spacing. This increased competition of laser modes has a simple qualitative explanation. Spatial structures of cavity eigenmodes most strongly overlap near a cavity mirror since loops of all modes meet there. How this effect is manifested depends quantitatively on the particular type of the longitudinal nonuniformity of the unsaturated gain.

The emergence of solid-state longitudinally pumped lasers renewed interest in specific features of their dynamical behavior caused by nonuniform gain profile inside the laser cavity. One cause of the longitudinal gain nonuniformity is that the cavity is filled by the active medium only partially. Another natural cause is the exponential absorption of the pump intensity when a pump beam propagates along the active element. The influence of each type of gain nonuniformity was studied separately in Refs. [3,4]. In Ref. [3], it was shown both experimentally and theoretically that the partial filling of a cavity by the active medium may lead to a suppression of the optical modes with a potentially large gain (for example, the central mode) by weaker modes. Analogous conclusions were drawn in the other work [4], where an exponential decrease in the population inversion from one end of the crystal (from which the laser is pumped) to the other was considered. The present paper reports an experimental and theoretical study of the joint effects of these two types between longitudinal gain nonuniformity on the competitive interaction of longitudinal modes. A detailed comparison of different approaches to the problem of describing the longitudinal gain nonuniformity is made.

II. MODEL OF SOLID-STATE DIODE-PUMPED LASERS

The behavior of multimode solid-state lasers is well described by the rate equations, which have been thoroughly studied for the case of uniform pumping [5–9]:

$$\frac{dI_k(\tau)}{d\tau} = GI_k(\tau)\left[g_k \int_0^L n(z,\tau)\psi_k^2(z)dz - 1 - \beta_k \right], \quad (1)$$

$$\frac{\partial n(z,\tau)}{\partial \tau} = A(z) - n(z,\tau)\left[1 + \sum\ g_j \psi_j^2(z) I_j(\tau) \right]. \quad (2)$$

Here the following dimensionless notations are used: $I_k(\tau)$ is the normalized intensity of an individual mode; $n(z,\tau)$ is the density of the population inversion; $\tau = t/T_1$ is the time measured in units of the inversion decay rate; z is a longitudinal coordinate; L is the cavity length; $A(z)$ is the pumping parameter, which reflects the unsaturated inversion distribution along the cavity; $\psi_k(z)$ is the resonator eigenfunction, and $\psi_k(z) = \sqrt{2}\sin(\pi q_k z/L)$ for longitudinal modes of a Fabry-Perot cavity; $\pi q_k/L$ is the wave number (where q_k is a large integer corresponding to the number of half-wavelengths of the kth mode in the cavity) and $k = 1,2,\ldots,K$, where K is the full number of laser modes included in the model; $G = T_1/T_c$, where T_c is the photon lifetime in the laser cavity; g_k is the kth mode gain coefficient; and β_k represents additional losses in the kth mode with respect to the loss rate of the reference level specified by $1/T_c$.

Therefore, the variables in Eqs. (1) and (2) are the mode intensities, which depend solely on time, and the population inversion, which depends also on the spatial coordinates. For this reason a partial derivative $\partial n/\partial \tau$ is used in Eq. (2). In the simplest case when the pump is uniform along the cavity $[A(z) = A_0]$, the transition from the integrodifferential equations to a set of ordinary differential equations is made by expanding the inversion into an infinite series

$$n(z,\tau) = D_0(\tau) - 2\sum_{k=1}^{K} N_k(\tau)\cos(2\pi q_k z/L) + \cdots \quad (3)$$

that takes into account only those terms of expansion (3) that are written out above, coefficients of which are directly included into equations for modal intensities. The dimension of this model is $2K+1$. Coefficients of this expansion are the population inversion averaged over the cavity length, and the amplitudes of spatial inversion gratings with the scale of nonuniformity of $\sim\lambda/2$, as induced by spatial hole burning

by each optical mode. Note that the commonly used Tang-Stalz-deMars model [6–9] does not cover large-scale Fourier components of population inversion with nonuniformity on the scale of $\sim L/2(q_i-q_j)$ as well as small-scale gratings with nonuniformity on the scale of $\sim\lambda/4$. These studies have shown that this approximation is quite valid to describe low-frequency dynamics of multimode solid-state lasers in case of a uniform gain distribution along the cavity.

In real lasers, however, the pumping of an active medium is not uniformly distributed along the cavity. At present, there are two alternative approaches to the problem of taking into account the nonuniformity of the unsaturated gain (population inversion) profile. The key difference between these approaches is a type of series expansion of the population inversion of the active medium in terms of functions $\cos(2\pi Q_i z/L)$ [2–4,10]. Here Q_i indicates both the small integer numbers $(0,1,2,\ldots,K-1)$ and large numbers coinciding with q_k.

In Ref. [2], the spatial gain nonuniformity (short active medium) was considered by substituting the integration over the entire cavity length in Eq. (1) for integration over the length of the active medium only, and by using expansion (3) for $n(z,\tau)$. As a result, additional terms (in comparison with the simplest case) appear in equations for the field intensities to describe changes in competing interactions of laser modes. The dimension of the model remains the same, $2K+1$. A weak point of this approach is the absence of strict substantiation of the validity of such change in the integration limits by using expansion (3) for $n(z,\tau)$, since eigenfunctions in expansion (3) are defined over the entire length of the cavity.

In Ref. [10], by introducing new variables in the expansion of the population inversion

$$n(z,\tau)=D_0(\tau)+2\sum_{p=1}^{K-1}D_p(\tau)\cos(2\pi pz/L)-2\sum_{k=1}^{K}N_k(\tau)\cos(2\pi q_k z/L) \tag{4}$$

as large-scale Fourier components $D_p(\tau)$, it was possible to take account of the unsaturated gain nonuniformity. In the first approach the dimension of the equations $2K+1$ is the same as for the uniform pumping, while the second approach leads to an increase in the dimension up to $3K$. In this paper we present a strict substantiation of the approach developed in Refs. [2–4] to describe the dynamics of solid-state lasers with nonuniformity of the gain caused jointly by the partial filling of a laser cavity by the active medium [2,3] and by the exponential absorption of the pump field along the active element [4]. Note that this problem is typical of class-*B* lasers only, which in the rate-equation approximation require that the differential connection (2) between the laser field and the population inversion should be considered. In class-*A* lasers the population inversion is adiabatically eliminated from the equations, while in class-*C* lasers the rate-equation approximation is invalid.

Here we should note once again that the aim of this paper is to present a justification of the multimode laser model used in Ref. [2–4], where the influence of the time-constant longitudinal nonuniformity of gain on inversion distribution along the cavity was divided into two parts. First, an unsaturated part of population inversion was singled out. This part repeats the longitudinal pump distribution and thus is time constant. So we can exclude the large-scale Fourier components of the inversion from the dynamic variables of the model. The other part of the inversion describes the effect of inversion saturation by the laser field. It can be seen in Eq. (2) that in steady state the saturated inversion distribution is proportional to the unsaturated gain $A(z)$:

$$\bar{n}(z)=A(z)\left[1+\sum g_j\psi_j^2(z)\bar{I}_j\right]^{-1}. \tag{5}$$

Here and further throughout this paper the stationary value of a variable will be noted with an overbar. It is quite natural, therefore, to introduce into consideration a new dynamical variable $Y(z,\tau)$ by representing the unsaturated gain profile as a separate time-constant cofactor in function $n(z,\tau)$:

$$n(z,\tau)=\Phi(z)Y(z,\tau). \tag{6}$$

Here $\Phi(z)$ with $A(z)=A_0\Phi(z)$ is determined only by the geometry of the problem (crystal size, exponential change of pumping along the crystal rod, etc.) and is responsible for slow changes in the population inversion along the cavity length. The new variable $Y(z,\tau)$ is responsible for the effect of saturation of the population inversion by the lasing field; note that in the absence of the field, $Y(z,\tau)=A_0$. Inserting Eq. (6) into Eqs. (1) and (2) yields

$$\frac{dI_k(\tau)}{d\tau}=GI_k(\tau)\left[g_k\int_0^L\Phi(z)Y(z,\tau)\psi_k^2(z)dz-1-\beta_k\right], \tag{7}$$

$$\frac{\partial Y(z,\tau)}{\partial\tau}=A_0-Y(z,\tau)\left[1+\sum g_j\psi_j^2(z)I_j(\tau)\right]. \tag{8}$$

Let us represent the separate multipliers in Eq. (6) as Fourier series in terms of rapidly oscillating functions for $Y(z,\tau)$ and slowly oscillating functions for $\Phi(z)$:

$$Y(z,\tau)=D_0(\tau)-2\sum_{k=1}^{K}Y_k(\tau)\cos(2\pi q_k z/L)-2\sum_{k=1}^{K}X_k(\tau)\sin(2\pi q_k z/L)+\cdots, \tag{9}$$

$$\Phi(z)=1+2\sum_{j=1}^{K}\Phi_j\cos(2\pi jz/L)+2\sum_{j=1}^{K}\Psi_j\sin(2\pi jz/L)+\cdots. \tag{10}$$

The following notations for the expansion coefficients $D_0(\tau)$, $Y_k(\tau)$, $X_k(\tau)$, Φ_j, Ψ_j are used:

$$D_0(\tau)=\frac{1}{L}\int_0^L Y(z,\tau)dz,$$

$$Y_k(\tau)=-\frac{1}{L}\int_0^L Y(z,\tau)\cos(2\pi q_k z/L)dz,$$

$$X_k(\tau)=-\frac{1}{L}\int_0^L Y(z,\tau)\sin(2\pi q_k z/L)dz, \tag{11}$$

$$\Phi_0=\frac{1}{L}\int_0^L \Phi(z)dz\equiv 1,$$

$$\Phi_j=\frac{1}{L}\int_0^L \Phi(z)\cos(2\pi jz/L)dz,$$

$$\Psi_j=\frac{1}{L}\int_0^L \Phi(z)\sin(2\pi jz/L)dz. \tag{12}$$

By substituting Eqs. (9) and (10) into Eq. (7), and taking into account that $\psi_k^2(z)=1-\cos(2\pi q_k z/L)$, we obtain K equations for the modal intensities. Then, integrating Eq. (8) over the cavity length, we obtain an equation for $D_0(\tau)$. Multiplying Eq. (7) by either $-\cos(2\pi q_k z/L)$ or $-\sin(2\pi q_k z/L)$ with subsequent integration over the cavity length leads to equations for $Y_k(\tau)$ and $X_k(\tau)$, respectively. Eventually, we obtain the following set of $3K+1$ equations:

$$\frac{dI_k}{d\tau}=GI_k\left[g_k\left(D_0+\sum_{m=1}^{K}(Y_m\Phi_{|k-m|}+X_m\Psi_{|k-m|})\right)-1-\beta_k\right], \tag{13}$$

$$\frac{\partial D_0}{\partial\tau}=A_0-D_0\left[1+\sum_{m=1}^{K}g_mI_m\right]-\sum_{m=1}^{K}g_mI_mY_m, \tag{14}$$

$$\frac{\partial Y_k}{\partial\tau}=-Y_k\left[1+\sum_{m=1}^{K}g_mI_m\right]-\frac{1}{2}g_kI_kD_0, \tag{15}$$

$$\frac{\partial X_k}{\partial\tau}=-X_k\left[1+\sum_{m=1}^{K}g_mI_m\right]. \tag{16}$$

Since the expression $(1+\Sigma_{m=1}^{K}g_mI_m)$ is always positive, it follows from Eq. (16) that all expansion coefficients X_k, regardless of the initial state in the limit of large time, will disappear and will not participate in the dynamics of a multimode laser. So the variables X_k may be set equal to zero and eliminated from the set of equation (13)–(16), and the coefficients Ψ_j in expansion (10) of function $\Phi(z)$ may be neglected. Thus the rate-equation model of a multimode solid-state laser with longitudinally nonuniform gain profile along the cavity length may be represented by the following set of ordinary differential $2K+1$ equations:

$$\frac{dI_k}{d\tau}=GI_k\left[g_k\left(D_0+\sum_{m=1}^{K}Y_m\Phi_{|k-m|}\right)-1-\beta_k\right],$$

$$\frac{\partial D_0}{\partial\tau}=A_0-D_0\left[1+\sum_{m=1}^{K}g_mI_m\right]-\sum_{m=1}^{K}g_mI_mY_m,$$

$$\frac{\partial Y_k}{\partial\tau}=-Y_k\left[1+\sum_{m=1}^{K}g_mI_m\right]-\frac{1}{2}g_kI_kD_0. \tag{17}$$

It should be emphasized that this approach considers the large-scale nonuniformity of the population inversion caused by the longitudinal nonuniformity of the pump. Expressions for these large-scale Fourier components are easy to obtain by substituting expansions (9) and (10) into Eq. (6):

$$D_p^0(\tau)=D_0(\tau)\Phi_p.$$

The upper index ''0'' at $D_p(\tau)$ indicates that these Fourier components describe an unsaturated large-scale inversion profile. In other words, the lasing modes do not participate in the formation of these Fourier components. This leads to the absence of amplitudes $D_p^0(\tau)$ among variables of the equations (17). The connection of these Fourier components with the Fourier components in expansion (4) used in Ref. [10] may be written in the following form:

$$D_p(\tau)=D_p^0(\tau)+\tilde{D_p}(\tau) \tag{18}$$

Here the component $\tilde{D_p}(\tau)$ is responsible for the saturation effect, taking into account that this component leads to an increase in the modal dimension up to $3K$ in Ref. [10]. This is the principal difference between the two approaches. When the components $\tilde{D_p}(\tau)$ are neglected, the model suggested here is of the same nature as Tang-Statz-deMars model [5], i.e., both are based on similar approximations.

To compare the experimental data with the theoretical results obtained with the developed model [Eq. (17)], we will analyze a concrete type of longitudinal nonuniformity caused by the exponential absorption of the pump field along a crystal that fills the laser cavity only partially, which corresponds to real experimental conditions:

$$\Phi(z)=\begin{cases}\alpha L\exp(-\alpha z)/[1-\exp(-\alpha l)], & 0\leqslant z\leqslant l\\ 0, & l<z\leqslant L.\end{cases} \tag{19}$$

Such a representation of the distribution function ensures the equality $\Phi_0=1$. Other coefficients of the expansion have the form

$$\Phi_p=\frac{1}{1+q^2p^2}\left(\frac{e^{\alpha l}-\cos(2\pi pl/L)}{e^{\alpha l}-1}+\frac{q^2p^2\alpha l}{e^{\alpha l}-1}\frac{\sin(2\pi pl/L)}{(2\pi pl/L)}\right), \tag{20}$$

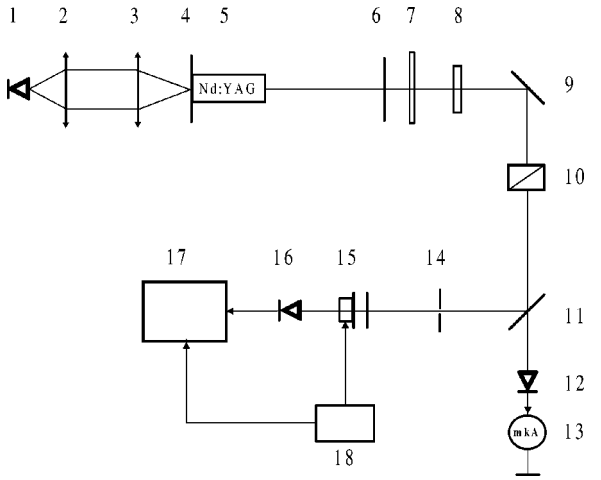

FIG. 1. Schematic of the experimental setup used in this study. (1) pump laser, 810 nm; (2 and 3) collimating lenses; (4 and 6) cavity mirrors; (5) yttrium aluminum garnet crystal; (7) filter $\lambda = 810$ nm; (8) $\lambda/2$ plate, $\lambda = 1064$ nm; (9 and 11) rotation mirrors; (10) Glan prism; (12 and 16) photodiodes; (13) microammeter; (14) aperture; (15) Fabry Perot spectrum analyzer; (17) oscilloscope; (18) scanning unit of a Fabry-Perot interferometer.

where $p = 1,2,\ldots,K-1$, $q = 2\pi/\alpha L$. Expression (20) transforms into the corresponding expressions of Ref. [4] (at $l \Rightarrow L$) or Refs. [2,3] (at $\alpha \Rightarrow 0$).

Results of numerical computation will be given below together with experimental results. Before presenting the experimental results we should make two comments. (i) The total number of modes K considered in model (17) includes both the lasing modes and the modes that for some reason have not entered the lasing process. In the simplest case of uniform pump distribution, such reason for this is that losses exceed the linear gain coefficient at the frequency of the considered mode. As a consequence, when the pump increases, all modes enter the laser process one after another, in series, starting from those nearest to the center of the gain line. At a constant pump, equations for modes with zero intensities may be excluded from the model. The situation is different in the case of longitudinal pump nonuniformity. It leads to such a change in the nonlinear mode coupling that modes with a potentially large gain cannot enter the lasing process, giving place to those modes that are farther from the center of the gain line. This results in a rarefaction of the optical spectrum. It is evident that in modeling this effect the equations for all modes located in the generation band must be considered. (ii) The results obtained with the two alternative approaches [the set of equations (17) and equations of Ref. [10]] in the domain of parameters for real experimental conditions fully coincide.

III. EXPERIMENTAL RESULTS

The experimental setup is shown schematically in Fig. 1. The pump source was semiconductor laser 1 that generated linearly polarized radiation at a wavelength of $\lambda = 810$ nm. The active element 5 was a 10-mm crystal rod, 6 mm in diameter with faces tilted at an angle of $\approx 1.5°$ relative to each other. The input face 4, being perpendicular to the rod axis, had a multilayer dielectric coating with ≈ 0.995 reflectivity at a wavelength of $\lambda = 1064$ nm and a relatively high transmission at the pump wavelength of 810 nm. The other crystal face had an antireflective coating at a wavelength of $\lambda = 1064$ nm. The output laser mirror 6 was a spherical mirror with ≈ 0.99 reflectivity and a radius of curvature of 30 cm. The experiment was carried out for two laser cavity lengths of 5.7 cm and 8.3 cm, giving filling factors of 0.32 and 0.22, respectively. The half-wave plate 8 and Glan prism 10 were used to study the optical spectrum of different polarization modes. Mode composition was monitored by the Fabry-Perot optical spectrum analyzer 15 with cavity lengths of 2.4 and 4.1 mm, which corresponded to free spectral ranges of ~ 63 and ~ 37 GHz, respectively. The fineness of the Fabry-Perot analyzer was $F = 119$.

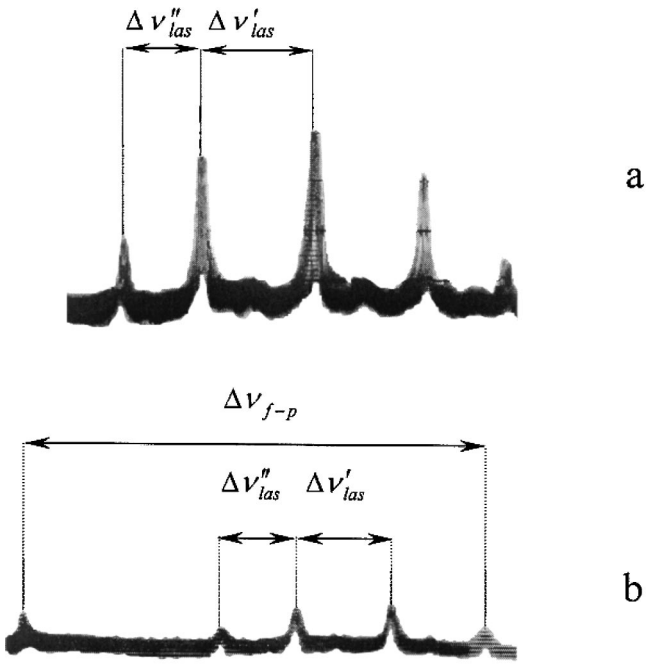

FIG. 2. Optical spectra for dominating polarization at $L_{opt} = 8.3$ cm (for two values of the pump parameter). (a) $A = 1.22$. (b) $A = 1.16$. $\Delta\nu'_{las}$ and $\Delta\nu''_{las}$ are frequency spacings between lasing modes; $\Delta\nu_{F\text{-}P}$ is free spectral range of the Fabry-Perot analyzer.

A quasi-isotropic Nd:YAG (yttrium aluminum garnet) laser cavity ensured a simultaneous lasing on two sets of orthogonally polarized longitudinal cavity eigenmodes. Linearly polarized pump radiation introduced discrimination into excitation conditions of the orthogonally polarized modes [11]. By means of a half-wave plate at $\lambda = 810$ nm (not shown in the figure), the orientation of the pump polarization was chosen such as to have a maximum discrimination of the polarization modes. So, in the emission spectrum, sets of ''strong'' and ''weak'' polarization modes were observed, which can be selected for study by means of the half-wave plate 8 and the polarizer 10.

Figure 2 is characteristic photos of the optical spectrum of strong polarization modes of a Nd:YAG laser at $L_{opt} = 8.3$ cm ($\Delta\nu = c/2L_{opt} = 1.8$ GHz). This figure shows that

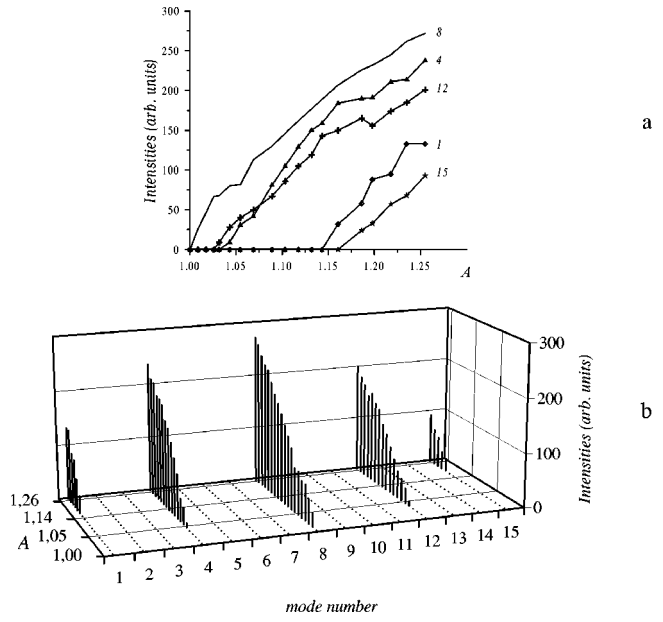

FIG. 3. Modal intensities vs pump parameter A [(a) two-dimensional presentation, (b) three-dimensional presentation] for $L_{opt}=8.3$ cm. 1,2, . . . ,15 show the numbers of cavity modes.

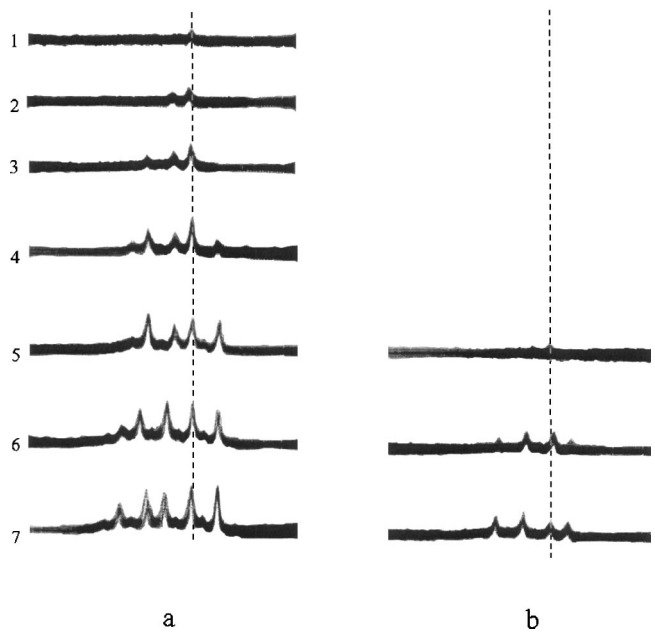

FIG. 4. Dynamics of the optical spectrum when the pump parameter A is increased for $L_{opt}=5.7$ cm. (a) Strong polarization mode. (b) Weak polarization mode.

the optical spectrum is nonequidistant. The frequency spacing between the central mode and the nearest modes $\Delta\nu'_{las}$ is larger than between two pairs of lateral modes $\Delta\nu''_{las}$. The frequency spacing between the lasing modes was compared with the free spectral range of the Fabry-Perot spectrum analyzer ($\Delta\nu_{F\text{-}P}=37$ GHz [see Fig. 2(b)]. With allowance for measurement error, the distance between the lasing modes was $\Delta\nu''_{las}=5.6\pm0.7$ GHz and $\Delta\nu''_{las}=7.4\pm0.9$ GHz. This approximately corresponds to three ($1.8\times3=5.4$ GHz) and four ($1.8\times4=7.2$ GHz) elementary longitudinal mode spacings $\Delta\nu$. This means that two or three longitudinal modes were suppressed between the lasing modes. Figure 3 shows the behavior of modal intensities versus pump parameter in the usual two-dimensional form [Fig. 3(a)] and in a three-dimensional presentation [Fig. 3(b)]. In the latter case, the position of the lasing modes on the frequency axis, with account of the frequency spacing between them (in units of the elementary longitudinal mode spacing $\Delta\nu$), is shown schematically. The numbers of longitudinal modes of the laser cavity (1,2, . . . ,15) are indicated along one axis in the horizontal plane (the frequency axis), and the pump parameter A along the other axis. The pump parameter was varied from $A=1.0$ to 1.3. Along the vertical axis the intensity of the lasing modes is given in arbitrary units. The plots show that at pump close to threshold only one mode is oscillating (mode number 8). When the pump is increased, the lateral mode Nos. 12 and 4 at a distance of four longitudinal mode spacings from the central mode, and then the lateral modes Nos. 1 and 15 at a distance of three longitudinal mode spacings from the adjacent mode Nos. 4 and 12, almost simultaneously enter the lasing process. Figure 3 shows that the intensities of all lasing modes nearly monotonically increase with increasing pump. Hopping between modes with adjacent longitudinal indices was practically unobserved in the experiment. The spectrum was almost symmetric and stable.

A series of analogous measurements was carried out for a shorter cavity length of $L_{opt}=5.7$ cm ($\Delta\nu=c/2L_{opt}=2.6$ GHz). The optical spectrum of a Nd:YAG laser was monitored by a Fabry-Perot optical spectrum analyzer with cavity length of 2.4 mm, which corresponds to mode spacing of 63 GHz. The width of the reference mode was close to 0.5 GHz. Figure 4(a) shows the optical spectrum of a strong polarization mode when the pump parameter is changed from $A=1.0$ to 1.5. The number of modes participating in the lasing was varied from 1 to 5. One can see that the optical spectrum is nonequidistent. Side modes enter the lasing process asymmetrically: when the pumping increases the center of the optical spectrum shifts to the low-frequency region (left). The intervals between the lasing modes were 4.8 ± 0.6 and 7.8 ± 0.9 GHz, which approximately correspond to two ($2.6\times2=5.2$ GHz) and three ($2.6\times3=7.8$ GHz) elementary longitudinal mode spacings $\Delta\nu$, respectively. This means that one or two longitudinal modes were suppressed between two lasing modes. Three-dimensional Fig. 5 shows the intensities of lasing modes versus the pump parameter, taking into account the position of the modes on the frequency axis. An analogous behavior of the weak polarization longitudinal modes is seen in Fig. 4(b). In this figure the lasing threshold for a weak polarization mode is $A=1.3$. The number of longitudinal modes in weak polarization is smaller than in strong polarization, but frequency spacings between lasing modes in this polarization coincide with those in strong polarization. Note that in contrast to the case of a long laser cavity, in this configuration the optical spectrum showed a considerable instability for both polarizations. This was manifested by frequent hopping from one longitudinal mode to adjacent modes. A reason for this may be that under these conditions the laser is more sensitive to uncontrolled experi-

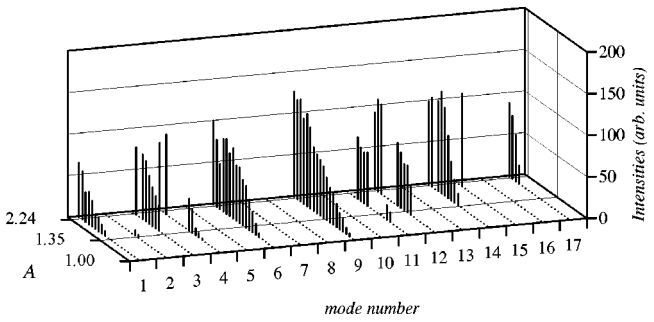

FIG. 5. Modal intensities vs pump parameter A (three-dimensional presentation) for $L_{opt}=5.7$ cm. 1,2, . . . ,17 show the numbers of cavity modes.

mental changes in the cavity length. Figure 5 shows a nonmonotonical change in the intensities of lasing modes versus the pump parameter.

Thus the results of our experimental study of the optical spectrum of a Fabry-Perot Nd:YAG laser with a thin active medium that is close to the input mirror of the cavity (filling factors 0.2 and 0.3) are as follows. The optical spectrum is significantly rare. Frequency spacings between modes vary from two to four longitudinal mode spacings $\Delta\nu$ of the cavity. A decrease in the filling factor leads to a greater rarefaction of the optical spectrum. Lasing modes become more stable to external perturbations and the competing influences of adjacent longitudinal modes.

IV. COMPARISON OF EXPERIMENTAL RESULTS WITH THE THEORY

To compare results of the theoretical study with experimental data, model (17), in the limit of 20 modes which could participate in the lasing process, was numerically integrated. Considering a Lorentzian gain profile, the gain coefficients can be written as

$$g_k=\left\{1+\left[\left(\frac{K}{2}+1-k\right)\delta-\delta_0\right]^2\right\}^{-1},$$

$$k=1,2,\ldots,K \quad (K=20),$$

where δ and δ_0 are the longitudinal mode spacing and the detuning of the mode nearest to the center of the gain line ($k=11$) from the line center, respectively, normalized to the halfwidth of the gain spectrum. Taking $\sim$160 GHz (135 GHz [12] to 195 GHz [13]) for the gain linewidth, under conditions of our experiment we obtain $\delta=0.021$ ($L_{opt}=8.3$ cm) and $\delta=0.03$ ($L_{opt}=5.7$ cm). To have a situation of asymmetry when all modes have different gain coefficients, in numerical calculation we introduce the detuning $\delta_0\approx\delta/4$. The literature gives different data for the absorption coefficient α ranging from 3 to 8 cm^{-1} [14] at a wavelength of 808 nm. Our measurements of the parameter α were from 3 to 4.5 cm^{-1}. One reason for such spread in values may be temperature changes in the semiconductor laser with the changing current of the laser diode, which causes a shift of the oscillation frequency. In numerical integration of the set of equations (17), we assumed $\alpha l=3.5$.

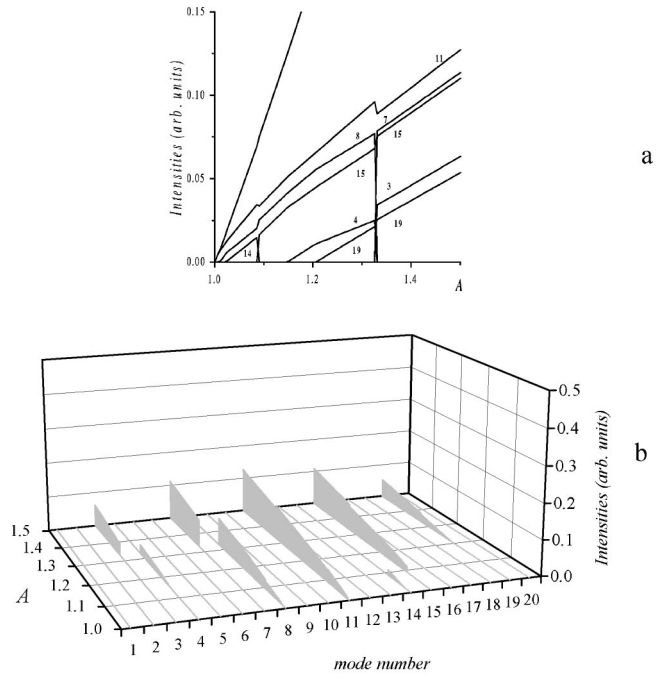

FIG. 6. Theoretical dependencies of the modal intensities on the pump parameter A [(a) two-dimensional presentation, (b) three-dimensional presentation] for $G=2500$, $l/L=0.22$, $\delta=0.021$, $\delta_0=\delta/4$, and $\alpha=3.5$ cm^{-1}.

Figures 6 and 7 show the results of numerical computation of the behavior of the modal intensities when the pump parameter is varied for two filling factors. Comparison of these results with corresponding experimental Figs. 3 and 5 shows

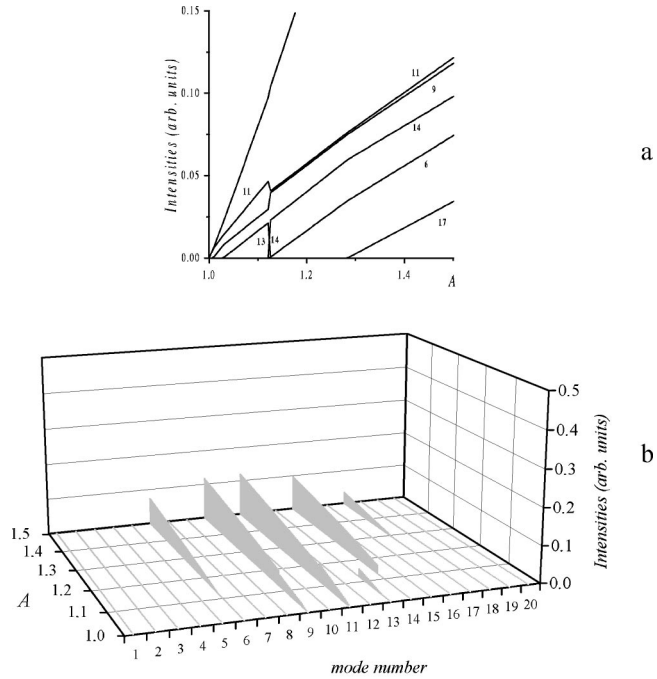

FIG. 7. Theoretical dependencies of the modal intensities on the pump parameter A [(a) two-dimensional presentation, (b) three-dimensional presentation] for $G=2500$, $l/L=0.32$, $\delta=0.030$, $\delta_0=\delta/4$, and $\alpha=3.5$ cm^{-1}.

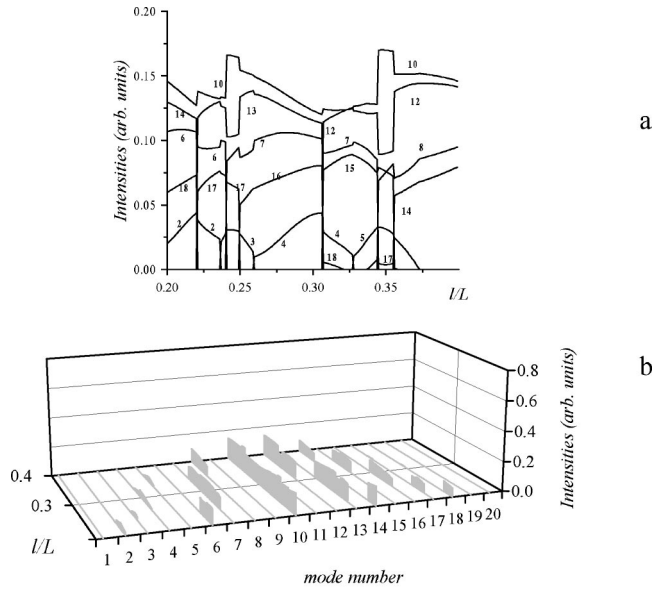

FIG. 8. Theoretical dependencies of the modal intensities on the filling factor l/L [(a) two-dimensional presentation, (b) three-dimensional presentation] for $G=2500$, $A=1.5$, $\delta=0.030$, $\delta_0=\delta/4$, and $\alpha=3.5\ \mathrm{cm}^{-1}$.

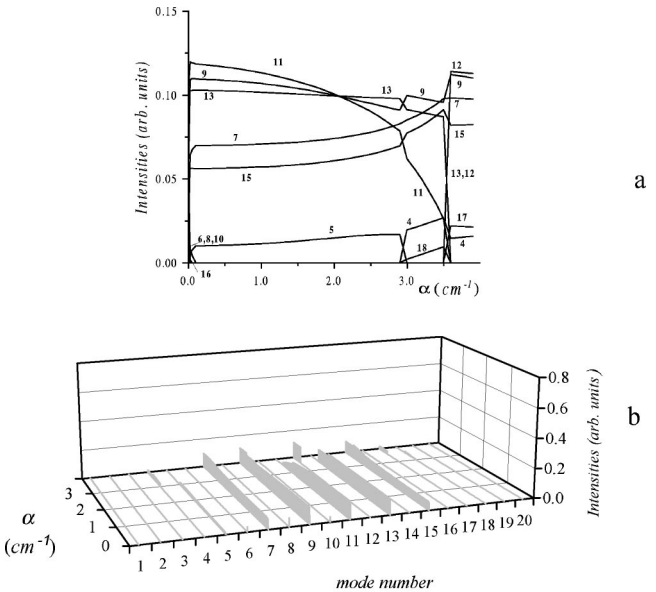

FIG. 9. Theoretical dependencies of the modal intensities on the absorption coefficient α [(a) two-dimensional presentation, (b) three-dimensional presentation] for $G=2500$, $A=1.5$, $l/L=0.22$, $\delta=0.021$, and $\delta_0=\delta/4$.

that the developed model (17) quite accurately describes the dynamics of the optical spectrum of a multimode solid-state laser with a nonuniform longitudinal pump profile, initially, as regards the frequency spacing between lasing modes. A decrease in the filling factor results in an increase in the frequency spacing between lasing modes, in excellent accordance with experiment. Moreover, at the pump absorption coefficient chosen for calculations there is a coincidence with the number of suppressed modes between lasing modes. In addition, the figures clearly demonstrate that changes in the pumping lead to hopping on adjacent longitudinal modes. This may also be one of the reasons (together with technical fluctuations of laser parameters, for example, the cavity length) for the hopping of modes observed in the experiment. In Fig. 8 the behavior of the mode intensities is calculated when the filling factor is varied. A real situation is modeled when changes in the filling factor are caused by changes in the cavity length. The change in the filling factor l/L is accompanied by proportional changes in the longitudinal mode spacing δ. The figure shows that when l/L is decreased, a larger number of longitudinal cavity modes enter the lasing process. But the number of lasing modes is practically constant, and the distance between the lasing modes increases (in units of intermode spacings). In Fig. 8 this distance is from two to four intermode spacings. Taking into account that a twofold decrease in the filling factor is accompanied by a twofold decrease in the intermode spacing, one can see that the total emission bandwidth is weakly changed. When analyzing Fig. 8, it is important to note that at $l/L\sim0.2$ all 20 modes for which model (17) is written participate in the lasing process. The figure shows that any further decrease in l/L should lead to a further broadening of the optical spectrum. But this cannot be demonstrated because, for simplicity, we have limited the model to 20 modes. Thus there is no sense in considering filling factors less than 0.2. The character of the influence of the exponential absorption of the pump radiation on the optical spectrum is exhibited in Figs. 9 and 10. These figures present the dynamics of the optical spectrum when the absorption coefficient α is changed at two values of the filling factor (0.22 and 0.32) realized in the experiment. It is evident that the appearance of the exponential absorption ($0<\alpha<0{,}1$) leads to a sharp rarefaction of

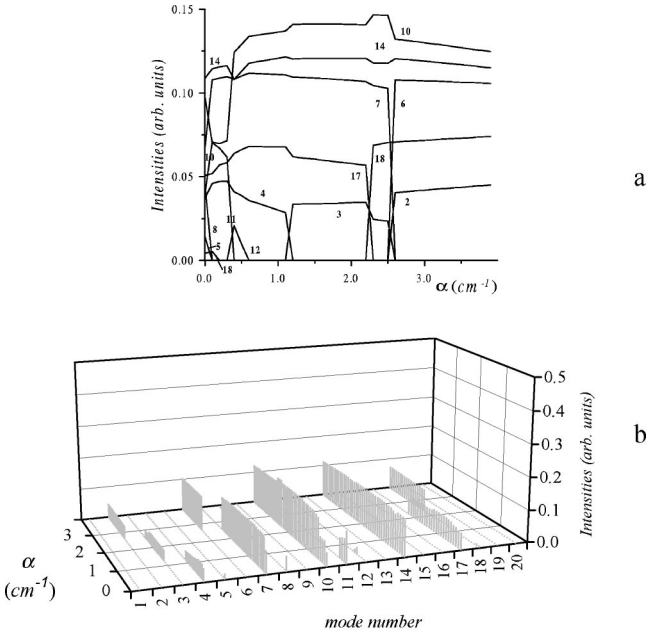

FIG. 10. Theoretical dependencies of the modal intensities on the absorption coefficient α [(a) two-dimensional presentation, (b) three-dimensional presentation] for $G=2500$, $A=1.5$, $l/L=0.32$, $\delta=0.030$, and $\delta_0=\delta/4$.

the optical spectrum. A further increase in α is accompanied by abrupt hops between some adjacent modes, with jumps in the intensities of lasing modes. Note that, in the absence of the exponential pump nonuniformity ($\alpha=0$), the changes in the filling factor are accompanied by nonmonotonical changes in the modal intensities, but that there are still no intensity jumps. The same is true in the case of an entirely filled laser cavity ($l/L=1$): changes in α are not accompanied by intensity jumps. Thus jumps in the modal intensities including hops of adjacent modes are characteristic only of the joint action of these two mechanisms of the longitudinal nonuniform pump profile along the laser cavity. Figures 9(b) and 10(b) demonstrate that the most suitable value for α is within $2\ \mathrm{cm}^{-1}<\alpha<4\ \mathrm{cm}^{-1}$, which is in good agreement with values measured in experiment.

V. DISCUSSION AND CONCLUSIONS

The experimental study of the optical spectrum of a solid-state laser has shown that a decrease in the filling factor from 0.32 down to 0.22 leads to a rarefaction of the optical spectrum: the number of suppressed modes between adjacent lasing modes increases from 1–2 to 2–3, respectively. The specific features of the optical spectrum observed in the experiment are easily explained by the developed model.

In this paper we have presented a model of a solid-state laser with a Fabry-Perot cavity which takes account of nonuniform pump distribution along the laser length caused both by the pump decay along the crystal and by a partial filling of the laser cavity by the active element. The suggested model is developed in an approximation commonly used for the case of uniform pumping which neglects the influence of large-scale Fourier components of the inversion $D_p^{\sim}(\tau)$ induced by saturation of the lasing modes. In the model discussed herein, large-scale Fourier components of the inversion induced by the longitudinal nonuniform pump profile (unsaturated part of the population inversion) are considered by introducing additional terms in equations for modal intensities in comparison with the simplest case of a uniform pump profile. In this approach, the dimension of the model remains the same $(2K+1)$ as in the case of uniform longitudinal pump.

Numerical computation of the model suggested in Ref. [10] has shown that, first, the behavior of the intensities coincides with that calculated according to the developed model [Eq. (17)] and, second, the order of magnitude of the stationary amplitudes of components $\overline{D_p^{\sim}}=\overline{D}_p-\overline{D}_0\Phi_P$ remains $(0.01,\ldots,0.03)\times\overline{D}_0$ both in the absence of nonuniform pump distribution ($l/L=1$ and $\alpha=0$), as well as in the whole range of parameters l/L and α where the approximation of 20-mode lasing is valid. These calculations show the validity of this approximation for finding steady state solutions and studying low-frequency dynamics of solid-state lasers.

In the experiment, lasing on orthogonally polarized modes was observed. Our study showed that the polarization interaction of modes does not affect the phenomenon of rarefaction of the spectrum in a multimode solid-state laser. The validity of this statement is seen in Fig. 4. Photos 1–4 are taken at a low pump level at which the orthogonally polarized modes have not yet entered the lasing process. In these circumstances the polarization interaction of modes has no effect on the rarefaction of the optical spectrum. The polarization interaction of modes is manifested as additional relaxation oscillations only in low frequency dynamics [11,15].

It is important to note that the linearly polarized radiation of a pump laser leads to a polarization nonuniformity of the pumping [11,15] which has an effect on the character of the polarization modal interaction. Obviously, to describe specific features of multimode lasing of a bipolarized solid-state laser, it is more convenient to use, as a starting model, a model with an initially lower dimension, since the introduction of a set of orthogonal modes and angular harmonics of the population inversion will significantly increase the modal dimension (approximately by four times [11,15]).

The developed model [Eq. (17)] offers the possibility to search analytically for steady-state solutions: the procedure of finding steady states when only an exponential decay of the pumping along the crystal is considered was suggested in Ref. [4]. Generalization to the case of an arbitrary longitudinal pump nonuniformity does not meet any difficulties in principle.

ACKNOWLEDGMENTS

The authors are thankful to Ya. I. Khanin for criticism and fruitful discussions. The work was carried out with the financial support of the Russian Foundation for Basic Research (Grants Nos. 96-02-19274 and 96-15-96742).

[1] E.S. Kovalenko, Izv. Vyssh. Uchebn. Zaved. Radiofizika **10**, 1765 (1967) [Sov. Radiophys. **10**, 989 (1967)]; E.S. Kovalenko and L.I. Shangina, *ibid.* **12**, 846 (1969) [*ibid.* **12**, 674 (1969)]; A.A. Gusev, S.V. Kruzhalov, L.N. Pakhomov, and V.Yu. Petrun'kin, Pis'ma Zh. Tekh. Fiz. **4**, 1250 (1978) [Sov. Tech. Phys. Lett. **4**, 503 (1979)]; V.R. Mironenko and V.I. Yudson, Opt. Commun. **41**, 126 (1982); K.N. Evtyukhov, L.N. Kaptsov, and I.V. Mitin, Zh Prik. Spektrosk. **32**, 18 (1980) [J. Appl. Spectrosc. **32**, 10 (1980)]; E.A. Viktorov, V.A. Sokolov, E.V. Tkachenko, and V.I. Ustyugov, Opt. Spektrosk. **68**, 920 (1990) [Opt. Spectrosc. **68**, 537 (1990)].

[2] O. Evdokimova and L. Kaptsov, Kvant. Elektron. **16**, 1557 (1989) [Sov. J. Quantum Electron. **19**, 1001 (1989)].

[3] N.B. Abraham, L. Sekaric, L.L. Carson, V. Seccareccia, P.A. Khandokhin, Ya.I. Khanin, I.V. Koryukin, and V.G. Zhislina, Phys. Rev. A (to be published).

[4] L Stamatescu and M.W. Hamilton (private communication).

[5] C.L. Tang, H. Statz, and G. de Mars, J. Appl. Phys. **34**, 2289 (1963).

[6] Ya.I. Khanin, *Principles of Laser Dynamics* (North-Holland, Amsterdam, 1995); Ya.I. Khanin, *Principals of Laser Dynamics* (Nauka, Moscow, 1999).

[7] P. Mandel, *Theoretical Problems in Cavity Nonlinear Optics* (Cambridge University Press, Cambridge, 1997).
[8] P.A. Khandokhin, Paul Mandel, I.V. Koryukin, B.A. Nguyen, and Ya.I. Khanin, Phys. Lett. **235**, 248 (1997).
[9] P.A. Khandokhin, Ya.I. Khanin, J.-C. Celet, D. Dangoisse, and P. Glorieux, Opt. Commun. **123**, 372 (1996).
[10] D. Pieroux and P. Mandel, Quantum Semiclassic. Opt. **9**, L17 (1997).
[11] P.A. Khandokhin, N.D. Milovsky, Yu.A. Mamaev, E.A. Ovchinnikov, E.Yu. Shirokov, in *Laser Optics'98: Solid State Lasers*, edited by V.I. Ustyugov [Proc. SPIE **3682**, 53 (1998)].
[12] W. Koechner, *Solid-State Laser Engineering*, 3rd ed. (Springer, Heidelberg, 1993).
[13] G.M. Zverev and Yu.D. Golyaev, *Crystal Lasers and Their Applications* (Radio i svyaz, Moscow, 1994).
[14] T.Y. Fan and L. Byer, IEEE J. Quantum Electron. **QE-23**, 605 (1987).
[15] P.A. Khandokhin, Ya.I. Khanin, Yu.A. Mamaev, N.D. Milovsky, E.Yu. Shirokov, S. Bielawski, D. Derozier, and P. Glorieux, Kvant. Elektron. **25**, 517 (1998) [Sov. J. Quantum Electron. **28**, 502 (1998)]; P. Khandokhin, Ya. Khanin, Yu. Mamaev, N. Milovsky, E. Shirokov, S. Bielawski, D. Derozier, and P. Glorieux, Quantum Semiclassic. Opt. **10**, 97 (1998).